IEEE Access
Multidisciplinary | Rapid Review | Open Access Journal

Received September 20, 2019, accepted September 29, 2019, date of publication October 4, 2019, date of current version October 16, 2019.

Digital Object Identifier 10.1109/ACCESS.2019.2945602

What Are Spectral and Spatial Distributions of EEG-EMG Correlations in Overground Walking? An Exploratory Study

JUNHUA LI[1,2,3,4], (Senior Member, IEEE), GEORGIOS N. DIMITRAKOPOULOS[2], PAVITHRA THANGAVEL[5], GONG CHEN[5], YU SUN[6], (Senior Member, IEEE), ZHAO GUO[7], HAOYONG YU[5], (Senior Member, IEEE), NITISH THAKOR[8], (Life Fellow, IEEE), AND ANASTASIOS BEZERIANOS[8], (Senior Member, IEEE)

[1]Laboratory for Brain-Bionic Intelligence and Computational Neuroscience, Wuyi University, Jiangmen 529020, China
[2]Singapore Institute for Neurotechnology (SINAPSE), National University of Singapore, Singapore 117456
[3]School of Computer Science and Electronic Engineering, University of Essex, Colchester CO4 3SQ, U.K.
[4]Centre for Multidisciplinary Convergence Computing (CMCC), School of Computer Science and Engineering, Northwestern Polytechnical University, Xi'an 710072, China
[5]Department of Biomedical Engineering, National University of Singapore, Singapore 117575
[6]Key Laboratory for Biomedical Engineering of Ministry of Education of China, Department of Biomedical Engineering, Zhejiang University, Hangzhou 310007, China
[7]School of Power and Mechanical Engineering, Wuhan University, Wuhan 430072, China
[8]N.1 Health Institute, National University of Singapore, Singapore 117456

Corresponding author: Junhua Li (juhalee.bcmi@gmail.com)

This work was supported in part by the National Natural Science Foundation of China under Grant 61806149, and in part by the Ministry of Education of Singapore under Grant MOE2014-T2-1-115.

ABSTRACT You probably believe that a latent relationship between the brain and lower limbs exists and it varies across different walking conditions (e.g., walking with or without an exoskeleton). Have you ever thought what the distributions of measured signals are? To address this question, we simultaneously collected electroencephalogram (EEG) and electromyogram (EMG) signals while healthy participants were conducting four overground walking conditions without any constraints (e.g., specific speed). The EEG results demonstrated that a wide range of frequencies from delta band to gamma band were involved in walking. The EEG power spectral density (PSD) was significantly different in sensorimotor and posterior parietal areas between exoskeleton-assisted walking and non-exoskeleton walking. The EMG PSD difference was predominantly observed in the theta band and the gastrocnemius lateralis muscle. EEG-EMG PSD correlations differed among walking conditions. The alpha and beta bands were primarily involved in consistently increasing EEG-EMG PSD correlations across the walking conditions, while the theta band was primarily involved in consistently decreasing correlations as observed in the EEG involvement. However, there is no dominant frequency band as observed in the EMG involvement. Channels located over the sensorimotor area were primarily involved in consistently decreasing EEG-EMG PSD correlations and the outer-ring channels were involved in the increasing EEG-EMG PSD correlations. Our study revealed the spectral and spatial distributions relevant to overground walking and deepened the understanding of EEG and EMG representations during locomotion, which may inform the development of a more human-compatible exoskeleton and its usage in motor rehabilitation.

INDEX TERMS Correlation distribution, exoskeleton-assisted overground walking, electroencephalogram (EEG), electromyogram (EMG), naturalistic overground walking, power spectral density (PSD).

I. INTRODUCTION

Walking is a basic activity in daily life, and involves multiple functions ranging from perception to execution. When an exoskeleton is used during walking, it directly affects the

The associate editor coordinating the review of this manuscript and approving it for publication was Zehong Cao.

lower limb where the exoskeleton is attached and indirectly affects the brain, which supervises the lower limb. The former effect may lead to alterations in muscular activity, while the latter effect may change brain activity. These effects can be utilized to promote motor rehabilitation as benefiting to restore the closed loop between the brain and muscles of the lower limb [1], [2].

Establishment of the closed loop between the brain and muscles of the lower limb is essential during walking. Specifically, the central nervous system (CNS) initiates movement intention and delivers it to the muscles through the peripheral nervous system. The muscles then execute the required movements accordingly and send feedback to the CNS. For instance, imagined or real hand movements induce desynchronization in the contralateral sensorimotor cortex and synchronization in the ipsilateral sensorimotor cortex [3]–[5], indicating an evident correlation between movement and brain activation. This desynchronization is also found in the central cortical area when the lower limb is engaged in walking on a treadmill [6]. It is broadly accepted that the main regions associated with walking are the primary motor cortex and the primary somatosensory cortex [7]. This association has also been observed using other neuroimaging modalities, such as functional magnetic resonance imaging [8]–[10] and functional near-infrared spectroscopy [11]. As described in the literature, the frequency representation of EEG signals recorded from these relevant regions varies under different walking conditions [6], [12], [13]. The alpha and beta bands show relatively consistent involvement in walking execution [12], [14]–[17]. In addition, a walking comparison study found that higher theta band power was observed during walking on a balance beam than during walking on a treadmill [18]. It has also been reported that amplitude modulation in the gamma band is related to gait phase [19], [20]. However, the walking-related information in the gamma band might be due to motion artifact contamination [21]. Motion artifacts can be detected using sophisticated methods [22], [23] and removed from EEG data so that their effects are excluded. A recent study reported that the appropriate sensor setup can mitigate motion artifact introduction into EEG at slow walking speeds [24]. Taken together, the above findings demonstrate that the manner in which each band is involved in walking has not yet been well established. Nonetheless, the existence of a close relationship between cortical activity and walking is confirmable. Hashimoto and his colleagues reported that significant EEG-EMG coherence was observed at the frequency range of $14 \sim 30$ Hz [25]. This coherence was increased when a stronger muscular contraction was performed [26].

Although great progress in corticomuscular research during locomotion was made in the past decades, the following areas of research are either unaddressed or require further investigation. First, EEG-EMG PSD correlations have not been explored using high-density channels covering the entire brain during walking with and without the use of an exoskeleton. Second, the extent of the involvement of each frequency band and each channel (including EEG and EMG channels) in the EEG-EMG PSD correlations have not yet been addressed. Third, to the best of our knowledge, almost all previous studies have used a treadmill for the walking experiments [6], [12], [17], [22], [27]–[29], with an exception of the study in [30]. This may restrict the participants and alter their normal walking postures [31], possibly leading to differences in observations when compared to the situation where the participant walks overground at a self-selected pace. Fourth, EEG and EMG data should be recorded under different walking conditions using identical experimental settings (like the setting in this study [30]). This includes the use of identical devices, physical environment, and participant groups. This is to ensure that the study's findings are not biased due to differences in experimental settings. The PSD representations of EEG and EMG data related to walking with and without the use of an exoskeleton must be further investigated using data recorded with identical experimental settings. In order to address the above gaps in research, we designed experiments consisting of naturalistic walking and exoskeleton-assisted walking and collected both EEG and EMG data using identical experimental settings for the different walking conditions from the same participant group. In this study, the PSD representations of both EEG and EMG were explored and the distributions of the EEG-EMG correlations based on spectral powers of gait cycles was illustrated. We hypothesize that (1) spectral power desynchronization is dominantly observed in the central region of the sensorimotor cortex, which corresponds to lower limb movements; (2) spectral powers of EEG and EMG derived from each gait cycle are related during walking and that there are different relationships during naturalistic walking and exoskeleton-assisted walking; and (3) EEG-EMG PSD correlations depend on frequency bands and channel locations.

II. MATERIALS AND METHODS

A. PARTICIPANTS

Thirty healthy individuals were recruited for this study through advertising on the campus of the National University of Singapore (NUS). Only male participants were recruited because (1) the exoskeleton was constructed for a specific range of height and weight in order to appropriately provide assistance; and (2) the strength of female participants is generally different from that of male participants, which may lead to bias. Three subjects were excluded from the study due to incomplete data recording. None of the participants had any history of major lower limb injury or known neurological or locomotor deficits. The participants had normal vision or corrected-to-normal vision. Their average age was 24 years with a standard deviation of 2.32 years. The average body mass index was 22.92 ± 2.76 (mean $\pm$ standard deviation).

This study was carried out in accordance with the recommendations of the Good Clinical Practice (GCP) and the Bioethics Advisory Committee (BAC) guidelines and the

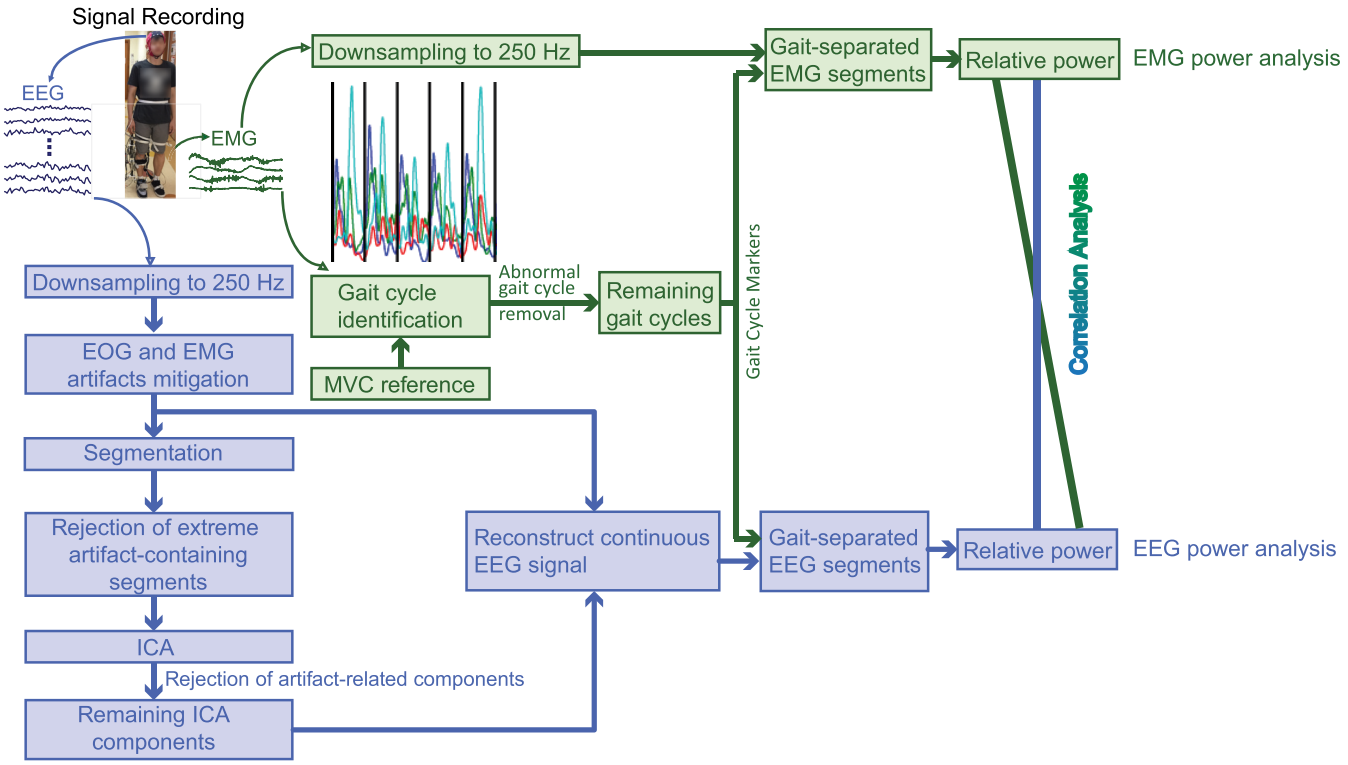

FIGURE 1. Schematic illustrating the EEG and EMG signal processing and their analyses. The EEG signal was partitioned into gait cycles after preprocessing, which consisted of downsampling, filtering, EOG and EMG artifacts mitigation, and ICA-based artifacts removal. Spectral power density was analyzed for both EEG and EMG segments. Their correlations were also investigated.

applicable laws and regulations of Singapore. The protocol was approved by the Institutional Review Board of the NUS, and all participants provided written informed consent.

B. EXOSKELETON

The unilateral exoskeleton used in this study was a compact and wearable robotic system that was optimized based on the biomechanics of human gait to provide suitable assistive torque for overground walking. The knee module was driven by a compliant force-controllable linear actuator featuring two sets of springs. The soft linear springs enabled the actuator to have high force control fidelity, low mechanical impedance, and true intrinsic compliance, while the torsional springs had a higher force control range and bandwidth [32]. In order to better synchronize the phases between the exoskeleton and the participants, a hidden Markov model was used to detect gait cycles, based on which an adaptive oscillator was implemented to estimate gait percentage. A predefined gait trajectory with 10% of phase leading was used to provide assistance with an impedance controller. The impedance controller was set to 0.2 Nm/deg to provide low assistive torque and to 0.4 Nm/deg to provide high assistive torque [33].

C. EXPERIMENTAL PROTOCOL

The participants were requested to perform four tasks: Zero Force (ZF, walking with an exoskeleton without torque assistance), Free Walk (FW, normal walking without exoskeleton support), Low Assistant Force (LAF, walking with an exoskeleton with low assistive torque), and High Assistant Force (HAF, walking with an exoskeleton with high assistive torque). The participants always performed the FW first, which was followed by the ZF. The order for performing LAF and HAF was randomized. The participants performed each task three times consecutively in a horizontal level corridor approximately 21 meters long and 2.1 meters wide. They were instructed to walk normally similar to their daily walking without any restriction (i.e., at a self-selected pace). A triple-deck trolley accommodating equipment and monitoring displayers was pushed by an experimenter who accompanied the participant alongside. The trolley was maintained at a proper distance to the participant (a picture of the experiment environment can be found in Fig. 1 in [34]). During the walking experiment, EEG, electrooculogram (EOG), and EMG were recorded using an ANT ASA-Lab system (ANT; Enschede, Netherlands). EEG data were collected using a WaveGuard EEG cap with 62 EEG channels (Eemagine GmbH; Berlin, Germany). The impedance of the EEG channel was maintained below 10 $k\Omega$. An additional EEG reference electrode was attached to the right earlobe. In addition, one bipolar EOG channel and four bipolar EMG channels were used. The positive and negative poles of the EOG channel were respectively placed in the supraorbital and infraorbital regions of the right eye.

Four bipolar EMG channels were placed on the surfaces of the major muscles connecting to the knee and ankle joints: tibialis anterior (TA), gastrocnemius lateralis (GL), rectus femoris (RF), and semitendinosus (SM). The placement of the EMG electrodes was in accordance with the suggestions by Criswell [35]. The centers of the two poles of the bipolar channel were 4.5 cm apart from each other. An alcohol swab saturated with 70% isopropyl alcohol was used to clean the skin surface before attaching the electrodes. The EMG electrodes were attached to the right lower limb, on which the exoskeleton was worn. All channels (i.e., EEG, EOG, and EMG channels) were simultaneously recorded at a sampling rate of 1,000 Hz. Before task implementation, a reference EMG record was collected while the participants voluntarily contracted their muscles to the maximal extent (i.e., maximal voluntary contraction, MVC). This recording was utilized to normalize the EMG signal. The normalization processing can mitigate differences in the force-generating capacities of various muscles, as well as differences across participants, as the force is expressed as a percentage of the MVC [36], [37]. The participants were allowed to practice to sufficiently acquaint themselves with walking while wearing the exoskeleton.

D. METHODS

An overview of the processing and analyses of the concurrent EEG and EMG signals is illustrated in Fig. 1. The EEG signals were first preprocessed to remove artifacts derived from eye and body movements etc., and then partitioned into segments according to gait cycles extracted based on the EMG signals. Analyses were performed for individual EEG and EMG signals, as well as for their PSD correlations.

1) PREPROCESSING

a: GAIT CYCLE IDENTIFICATION

Biomechanical data were not collected in the experiment. The gait cycles were therefore identified based on the EMG signals, as follows. After detrending and centering, a bandpass ($2 \sim 400$ Hz) filter was applied to the EMG signals using the function pop_eegfiltnew() in EEGLAB [38]. The filtered signals were then normalized using the reference record, expressed as a percentage of the maximum muscle activity recorded when the participant performed the MVC [36], [37]. The signal magnitude varied from one gait cycle to another, although the pattern of magnitude change was similar across the different gait cycles. We therefore utilized a peak detection method to partition continuous recordings into gait cycles [39]. Specifically, an in-house program for peak detection was used to calculate a threshold value dependent on the maximum and minimum values based on the combination of four EMG signals. The values above the threshold were detected as peaks. The intervals between the periodic peaks corresponded to gait cycles. After using this automatic gait cycle identification, a visual inspection was further conducted to adjust the partition of the gait cycles or to remove abnormal gait cycles. A gait cycle was identified as abnormal when its magnitude pattern did not follow the standard pattern. Extremely short or long gait cycles were also removed if their lengths were one standard deviation shorter or longer than the average length. 85.07%, 85.54%, 87.63%, and 87.56% of the originally collected gait cycles remained for ZF, FW, LAF, and HAF, respectively. The markers of the remaining gait cycles were stored for further use.

b: EMG PREPROCESSING

It is worth noting that the EMG data used for gait cycle identification were not directly used for data analysis after the processing steps. Instead, we analyzed the EMG data only after detrending and centering. The EMG data were first downsampled to 250 Hz, and then partitioned into gait cycles according to the gait cycle markers.

c: EEG PREPROCESSING

For each EEG channel, the amplitude mean was removed by subtracting the mean of each channel from the amplitudes of that channel. The EEG signals were then downsampled to 250 Hz and bandpass filtered ($0.5 \sim 45$ Hz) (using the functions in EEGLAB). This was followed by EOG mitigation. The effect of eye movements on EEG was mitigated using an adaptive filtering method [40]. The effect of EMG on the EEG was mitigated using a canonical correlation analysis-based method [41]. Subsequently, a continuous EEG signal was epoched into two-second segments. This was followed by segment rejection using EEGLAB toolbox [38]. The numbers of remaining segments were 54.3 ± 14.9, 46.8 ± 6.8, 51.2 ± 12.3, and 49.4 ± 9.6 for the ZF, FW, LAF, and HAF conditions, respectively. Independent component analysis using the infomax algorithm was utilized to decompose the remaining EEG segments into signal sources (i.e., independent components [ICs]). We obtained 62 independent components (equivalent to the number of EEG channels used for the decomposition). The ICs representing the remaining effects of EOG and EMG after the preceding EOG and EMG artifact mitigation or the pulse interference were removed. Examples of artefactual components are illustrated in Supplementary Figure S1. After the removal of artefactual ICs, the remaining ICs were then back-projected with the continuous EEG before the segmentation to reconstruct the continuous artifact-pruned EEG signal (see Fig. 1). The artifact-pruned EEG signal was then partitioned into gait cycles based on the gait cycle markers.

2) DATA ANALYSIS

Spectral power analysis was separately conducted for the EEG and EMG signals. A Fourier transform was applied to each gait cycle to estimate the frequency band powers. Frequency band powers were then transformed to log-space by computing ten times the base-10 logarithm of the powers for each frequency band ($10 \times \log_{10}{}^{Power}$). Five frequency bands (i.e., delta, $0.5 \sim 4$ Hz; theta, $4 \sim 7$ Hz; alpha $8 \sim 12$ Hz; beta $13 \sim 30$ Hz; and gamma, $31 \sim 45$ Hz) were analyzed for the EEG signal. The walking condition FW was

used as a baseline and the other three walking conditions with an exoskeleton were normalized by dividing corresponding powers at each frequency. The two-tailed t-test was employed to find channels on where frequency band powers of the walking conditions with an exoskeleton significantly differed from that of the walking condition without an exoskeleton. The significance level was adjusted by false discovery rate (FDR) to control the type I error. A total of six frequency bands (i.e., the above five frequency bands and an additional high-frequency band [100 $\sim$ 120 Hz]) were analyzed for the EMG signal. One-way repeated-measures analysis of variance (ANOVA) was used to determine whether there were significant spectral power differences between the walking conditions for each EMG channel and frequency band (4 channels $\times$ 6 frequency bands = 24). The false discovery rate (FDR) was used to correct for multiple comparisons. Statistical analyses were performed using Matlab software (Mathworks Inc., Version 8.6). In addition to the individual power analysis, the PSD correlations between EEG and EMG across the gait cycles was investigated. In order to eliminate potential interference due to varying power levels from one gait cycle to another, frequency band power was normalized through dividing by the sum of the five frequency band powers (i.e., delta, theta, alpha, beta, and gamma) to obtain relative power. We let e_i equal the spectral power of the ith gait cycle in a frequency band from an EEG channel and m_i equal the spectral power of the ith gait cycle in a frequency band from an EMG channel. The EEG-EMG PSD correlation r_{em} was obtained using the Pearson correlation, as follows:

$$r_{em} = \frac{\sum_{i=1}^{n} (e_i - \bar{e})(m_i - \bar{m})}{\sqrt{\sum_{i=1}^{n} (e_i - \bar{e})^2} \sqrt{\sum_{i=1}^{n} (m_i - \bar{m})^2}}, \quad (1)$$

where n was the number of gait cycles for a subject, $\bar{e}$ and $\bar{m}$ were the means of the spectral powers across all gait cycles for a subject, obtained as follows:

$$\bar{e} = \frac{1}{n} \sum_{i=1}^{n} e_i, \quad \bar{m} = \frac{1}{n} \sum_{i=1}^{n} m_i. \quad (2)$$

The PSD correlation calculation was repeated for each pair of EEG-EMG channels for all conditions (i.e., ZF, FW, LAF, and HAF), all frequency bands, and all subjects. This resulted in a total of 803,520 (62 EEG channels $\times$ 5 frequency bands $\times$ 4 EMG channels $\times$ 6 frequency bands $\times$ 4 conditions $\times$ 27 participants). Within all 803,520 EEG-EMG PSD correlations, non-significant EEG-EMG PSD correlations were screened out using the criterion of that their correlation values were not significant at the significance level of 0.05 (uncorrected), and then their correlation values were set to zero. Subsequently, the EEG-EMG PSD correlation values were averaged across participants after fisher z-transformation (including zeros). This resulted in 29,760 correlations (62 EEG channels $\times$ 5 frequency bands $\times$ 4 EMG channels $\times$ 6 frequency bands $\times$ 4 conditions). The average values of the EEG-EMG PSD correlations were then compared among the different conditions. We selected EEG-EMG PSD correlations whose average values were consistently increased or decreased across the different conditions (from ZF to HAF). Finally, we counted the number of times that each frequency band was involved in the remaining PSD correlations and explored their spatial distributions.

III. RESULTS

We separately analyzed the power spectral densities of the EEG and EMG signals, as well as their PSD correlations. We investigated the frequency bands and spatial distributions for significant EEG-EMG PSD correlations with consistent changes across the different conditions.

A. PSD ANALYSES

Fig. 2 depicts the topographies of PSD differences between the walking conditions with an exoskeleton (i.e., ZF, LAF, and HAF) and the walking condition without an exoskeleton (i.e., FW) in all five frequency bands. Red color indicates a higher PSD relative to FW while blue color indicates a lower PSD. The black dots stand for the channels with significant difference (FDR-corrected $p < 0.01$). The PSD was elevated in the beta and gamma bands over the sensorimotor and posterior parietal areas when assistance torque was provided when compared to FW. Higher assistance torque resulted in a larger increase in the PSD in the left posterior parietal region. In most cases, the PSD changes relative to FW is not unitary, showing the coexistence of increase and decrease in the PSD. Fig. 3 shows event-related spectral perturbation (ERSP) over gait cycle for a representative channel (i.e., Cz). We can see that ERSP was modulated across gait cycle for all walking conditions. The highest modulation appeared during ZF. The PSDs of each EMG channel and band were compared between conditions. The ANOVA results are presented in Fig. 4(A) (p-value was corrected using the FDR for multiple comparisons). As shown in Fig. 4(A), the dominant band and EMG channel involved in significant spectral power differences between the different conditions were the theta band and the GL channel (e.g., theta band in GL, $F(3,104) = 17.9$, $p < 0.0001$). A post-hoc two-tailed paired t-test revealed that spectral power differences between the different conditions were largely attributed to significant differences between FW and the other three conditions (see Fig. 4(B), e.g., ZF versus FW [$t(26) = 7.2$, $p < 0.0001$], FW versus LAF [$t(26) = -6.5$, $p < 0.0001$], FW versus HAF [$t(26) = -6.0$, $p < 0.0001$] in the theta band at channel GL). This indicates that the exoskeleton dramatically affected the spectral power representation in the EMG channels. Spectral power differences between walking conditions depended on frequency band and channel location. Delta band power during FW was higher than that during the other walking conditions at the GL and SM channels. Power was lower in the other bands during FW (see Fig. 4(B)).

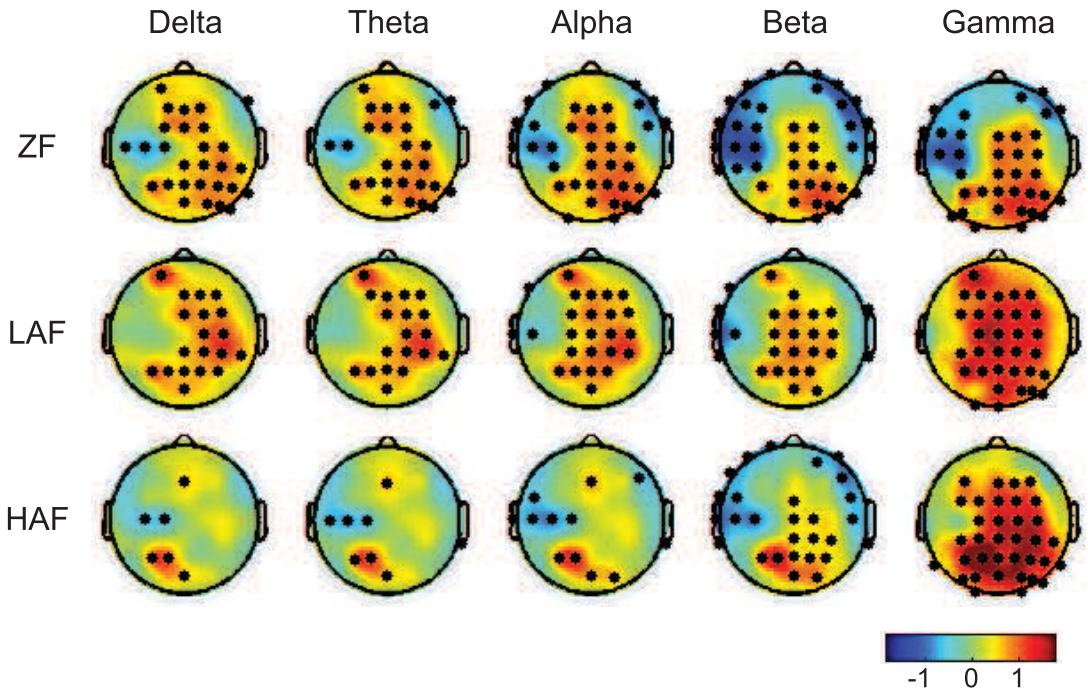

FIGURE 2. Topographies of power spectral density (PSD) differences between the walking conditions with an exoskeleton (i.e., ZF, LAF, and HAF) and the walking condition without an exoskeleton (i.e., FW) for all five frequency bands (i.e., delta, theta, alpha, beta, and gamma bands). Red color indicates a higher PSD relative to FW while blue color indicates a lower PSD. The black dots stand for the channels with significant difference (FDR-corrected $p < 0.01$).

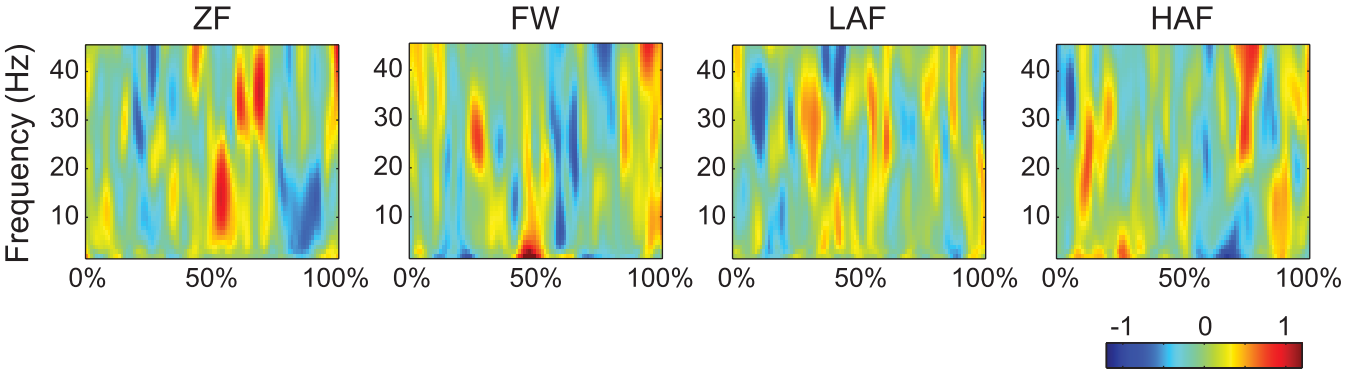

FIGURE 3. Time-frequency plots for four walking conditions at a representative channel (i.e., Cz), illustrating amplitude modulations relative to the full gait cycle baseline.

As shown in Fig. 5, the theta band in the EEG signal was predominant (equal to or greater than 25%) in the case of consistent decrease, while the alpha and beta bands were predominant in the case of consistent increase. However, no predominant band was found in the EMG signal for both cases of consistent decrease or increase. The spatial distributions of the consistently decreasing PSD correlations in EMG channels was relatively equal (see Fig. 6). In the case of consistently increasing PSD correlations, the TA channel was relatively predominant for the involvement in the correlations, while the SM channel was the least involved. When studying the spatial distributions of the EEG channels involved in the remaining PSD correlations, we found that the EEG channels over the sensorimotor area were mainly relevant to the consistently decreasing PSD correlations, and the outer-ring EEG channels located around the peripheral scalp were primarily involved in the consistently increasing PSD correlations (see Fig. 7). This spatial distribution was more obvious for channels that were ranked more highly. Although low EMG frequencies were included for analysis in some studies [42], [43], other researchers are of the opinion that these frequencies should be excluded [44]. In order to eliminate potential distortion due to low EMG frequencies in our analyses, we repeated the analyses after removing low

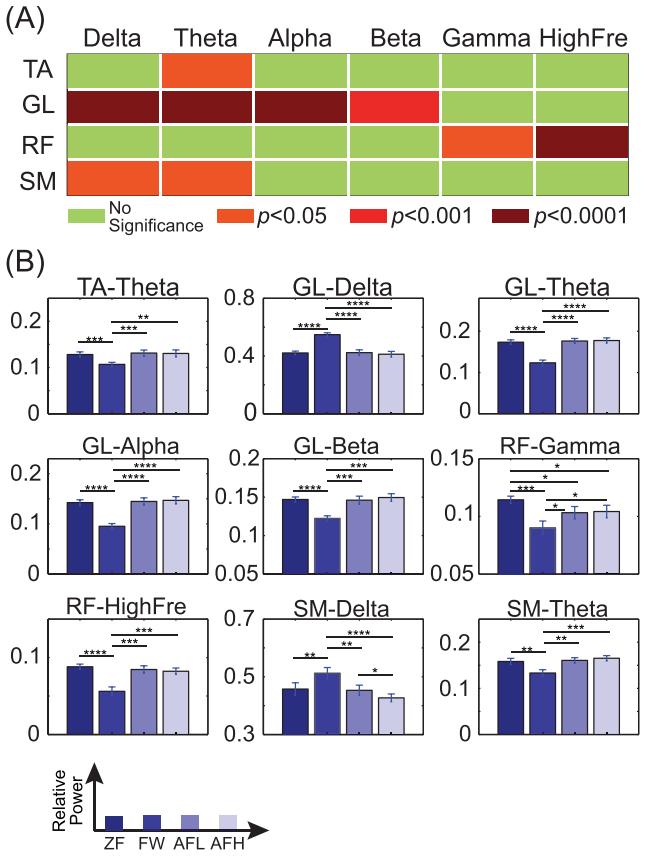

FIGURE 4. (A) ANOVA results for the four EMG channels (TA: tibialis anterior, GL: gastrocnemius lateralis, RF: rectus femoris, SM: semitendinosus) and six frequency bands. Light green color represents no significance, while the other colors represent different significance levels (after FDR correction for the multiple comparisons). (B) Means and standard errors of significant EMG power spectral densities, as determined using ANOVA (shown in non-green colors in the chart (A)). Asterisks illustrate post-hoc two-tailed paired t-test results (* $p < 0.05$, ** $p < 0.01$, *** $p < 0.001$, and **** $p < 0.0001$).

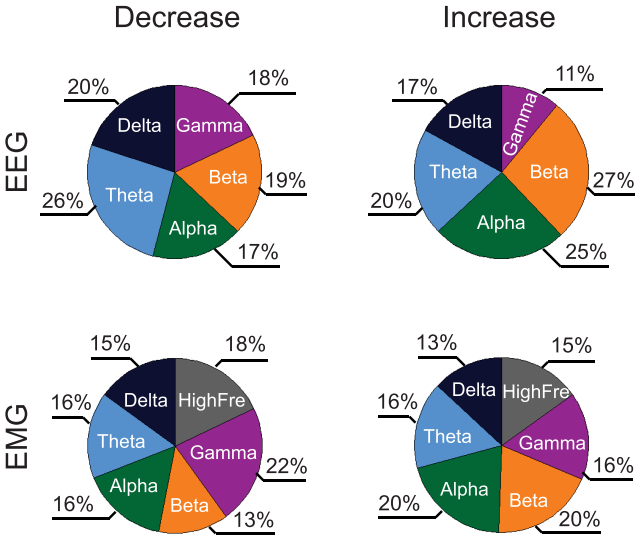

FIGURE 5. Occurrence (in percentage) of each band involved in consistently decreasing or increasing PSD correlations between EEG and EMG across the walking conditions. PSD correlations were calculated between EEG and EMG for each channel and each band, and then only significant correlations ($p < 0.05$, uncorrected) with consistent changes across the walking conditions were retained. The numbers of occurrences in these remaining PSD correlations for each band were counted and are reported as percentages.

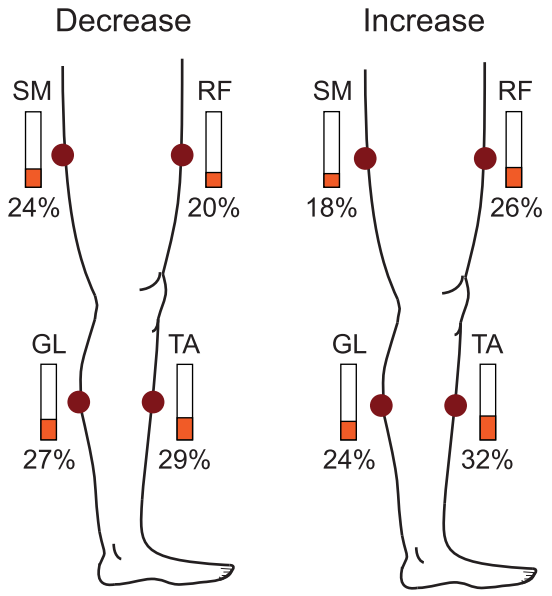

FIGURE 6. Occurrence (in percentage) of each EMG channel involved in consistently decreasing or increasing PSD correlations between EEG and EMG across the walking conditions. TA, GL, RF, and SM are abbreviations for tibialis anterior, gastrocnemius lateralis, rectus femoris, and semitendinosus, respectively.

EMG frequencies (i.e., delta and theta bands). The results are presented in Supplementary Figures S2, S3, and S4. These results did not reverse our findings.

IV. DISCUSSION

A. PSD ANALYSES OF EEG

The PSD analyses in this study demonstrated that a wide range of frequencies spanning from delta band to gamma band were involved in walking. This finding is agreement with the collective results derived from a batch of previous studies [12], [15], [16], [18]–[20], showing that the theta, alpha, beta, and gamma bands are related to walking. We found that PSD was significantly different when walking with an exoskeleton compared to walking without an exoskeleton, reflecting that the use of exoskeleton gave rise to PSD alteration during walking. Differences in PSD between different walking conditions were also observed in other experiments. The theta band power during balance beam walking differed from that during treadmill walking [18]. The extent of engagement to walking can modulate PSD in brain activities as concluded from a robot-assisted treadmill walking study, where the mu and beta band powers were more suppressed during active walking than passive walking [12]. Recently, the gamma band has also been shown to be involved in walking, as its oscillation is dynamically modulated in relation to the gait cycle [12], [16], [19]. This is in accordance

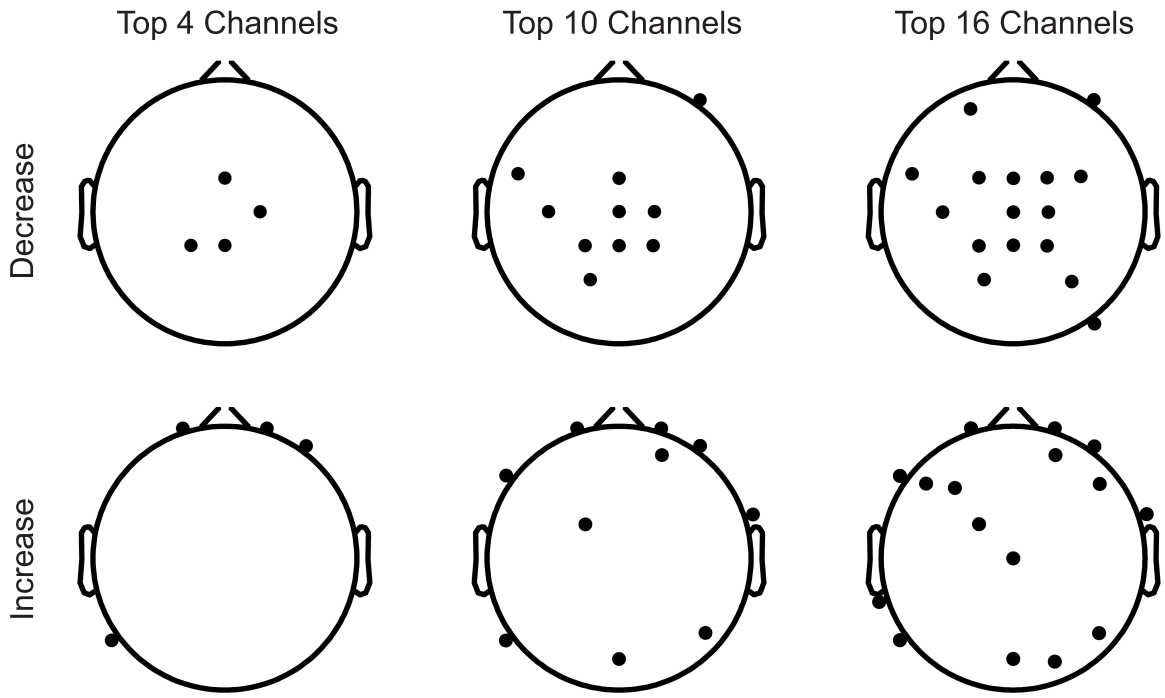

FIGURE 7. Spatial distributions of the top EEG channels (i.e., highest involvement in the EEG-EMG PSD correlation) involved in consistently decreasing or increasing PSD correlations between EEG and EMG across the walking conditions. The channels located over the sensorimotor area were predominantly involved in the decreasing PSD correlations and those scattered around the outer-ring area (i.e., around the peripheral scalp) were predominantly involved in the increasing PSD correlations.

with our finding of the involvement of gamma band in walking. In this study, we further revealed that the gamma band power was increased in sensorimotor and posterior parietal areas during walking with an exoskeleton compared to during walking without an exoskeleton. The enhancement of gamma band power was larger when higher force was provided to assist walking. Additionally, our study showed that delta band was modulated during walking. Prior to our work, features extracted from delta-band EEG signals have been utilized to decode kinematic and kinetic parameters of walking [28], [30]. As demonstrated in [30], the walking-related EMG can be decoded based on the delta band power of EEG. The relevance of the delta band to walking is further elucidated in our study, showing distinct differences between walking conditions depending on brain regions. Taken together, PSD was modulated in wide frequency range and multiple brain locations during walking and was differential between walking conditions. The findings in this study led us to speculate that an individual band modulation in particular brain region could underpin a certain neural process pertaining to walking and these individual band modulations collaboratively contribute to coordination and implementation of walking. For instance, the theta band modulation might underpin sensorimotor integration [45].

B. PSD ANALYSES OF EMG

The PSD of the EMG signal was significantly affected by the assistive exoskeleton. The majority of PSD comparisons over the different EMG channels and frequency bands showed an increase in PSD for conditions where an exoskeleton was used when compared to the condition where it was not used (see Fig. 4(B)). An increase in PSD when using the assistive exoskeleton was also found in another independent study [46]. However, we observed two exceptions in this study, where the power was decreased when using the assistive exoskeleton (i.e., GL-Delta and SM-Delta). Both exceptions appeared in the delta band, and may be due to soft tissue motion artifacts. In general, the effects of the exoskeleton on muscle activity depend on channel location and the frequency band. Based on the results of this study, an assistive exoskeleton mostly affects the GL muscle and the theta band power of EMG (see Fig. 4(A)). There were no significant differences in most of the power comparisons between conditions wherein an exoskeleton was used. This signifies that great care is required when the EMG signal is used to distinguish different levels of exoskeleton-based assistance. The EMG channel and the frequency band should be carefully selected when using EMG to distinguish conditions wherein an exoskeleton is worn because only very few cases with specific channels and specific frequency bands exhibit significant power differences, as shown in this study. Of note, the above findings were obtained based on aggregated power analyses averaged across all gait cycles and all time points for each gait cycle. Differential characteristics between different conditions wherein an exoskeleton is worn may exist in some time phases of the gait cycle.

C. DISTRIBUTION OF EEG-EMG PSD CORRELATIONS

The frequency bands and spatial distributions of significant EEG-EMG PSD correlations were explored in this study. We found that frequency bands in the EEG were not equivalently involved in the EEG-EMG PSD correlations. Furthermore, the predominantly involved bands were not identical for the cases of consistently decreasing and increasing PSD correlations. In the case of consistently decreasing PSD correlations, the theta band was predominant. The predominant bands were the alpha and beta bands in the case of consistently increasing PSD correlations. Taken together, these results indicate that the PSD correlation between the EEG and EMG was modulated across the walking conditions, and that this modulation was different at different frequency bands. The contrasting modulations for different frequency bands were also found in the amplitude as reported in previous studies [20], [47]. In addition, the predominant involvement of the beta band in the EEG-EMG PSD correlation in this study corroborated the results of a previous study reporting that the beta band is involved in the relationship between EEG and EMG during motor execution [25], [48], [49]. As reported by Seeber et al., amplitude was conversely modulated in the high and low gamma bands during walking, as indicated by the time-frequency exploration of gait cycles [20]. It was decreased in the alpha and beta bands and increased in the high gamma band during movements of the upper limb (e.g., finger movements) [47]. This opposite modulation (i.e., increase vs. decrease) existed not only in amplitude, but also in the relationship between the EEG and EMG PSDs, as indicated by the results of this study. We found that the EEG PSD changed along with the EMG PSD over gait cycles, and that the relationship between EEG and EMG underwent opposing changes across the walking conditions depending on the frequency band. Increased assistive torque was associated with increased cross-frequency correlation between EEG PSDs in the alpha and beta bands and EMG PSDs. This suggests that brain activity at the alpha and beta bands was more correlative with muscular activity over gait cycles. In the theta band of the EEG, the PSD correlation with the EMG data was decreased when there was an increase in assistive torque. This reflects a weakening of the relationship between brain activity at the theta band and muscular activity. In contrast to our observations for the EEG bands, we did not find any EMG band that was predominantly involved in either consistently decreasing or consistently increasing EEG-EMG PSD correlations. As observed in this study, the direction of the EEG-EMG PSD correlation was reversed (changed from positive to negative correlation, and vice versa) in walking conditions without assistive torque when compared to walking conditions with assistive torque. This demonstrates that the EEG-EMG PSD correlation was affected by the assistive torque provided by the exoskeleton. The coexistence of the opposing changes in the EEG-EMG PSD correlation indicates that the relationship adjustment between the EEG and EMG was not singular. Both increasing and decreasing changes in the EEG-EMG PSD correlations might play important roles in the incorporation of assistive torque into the loop between the brain and the lower limb when assistive torque is introduced into the loop. The direction of the EEG-EMG PSD correlation in the different walking conditions depended on the locations of the muscles and the brain regions. Based on our exploration of the EMG channels involved in the consistent EEG-EMG PSD correlations, the TA channel was predominantly involved in the consistently increasing EEG-EMG PSD correlations. This is in line with the previous observation of EEG-EMG coherence at the TA channel [25], [50]. They only used one EMG channel and had not explored the other EMG channels as employed in this study. We speculate that the spatial distribution might be related to the mechanism underlying the changes in drive from the human brain to lower limb muscles under the different walking conditions. The spatial distribution of the EEG channels indicate that the channels located over the sensorimotor area (e.g., C2) were predominantly involved in the decreasing EEG-EMG PSD correlations and that the channels scattered around the outer-ring area (i.e., around the peripheral scalp) were predominantly involved in the increasing EEG-EMG PSD correlations (see Fig.7). This phenomenon was more conspicuous for channels ranked as more involved in the PSD correlation. For instance, the top four channels involved in the decreasing PSD correlations were located at the midline sensorimotor area, which has repeatedly been found to be associated with walking [6], [7]. There has thus far been no report regarding the association between outer-ring channels and walking. The underlying mechanism of this association is not clear and requires further study. We speculate that this association may be related to the coordination between the processing of the perceived gait posture and the reactions of the muscles.

D. LIMITATIONS AND CONSIDERATIONS

This study has a few limitations. Biomechanical data, such as walking speed and acceleration, were not recorded. As a result, the EEG and EMG signals cannot be analyzed in relation to biomechanical data. The upper limbs usually swing along with the movements of the lower limbs. Due to the absence of biomechanical data recorded from the upper limbs, we were unable to probe the effect of upper limb movement. We have presented the PSD results after correction for multiple comparisons, but did not correct the p-values for the EEG-EMG PSD correlations. This is because the p-values for the EEG-EMG PSD correlations were not directly presented as results and underwent further processing. In contrast, the ANOVA results were presented directly. When exploring the EEG-EMG PSD correlations, p-values were used to screen out meaningful correlations at the first step. A further screening criterion was imposed to select correlations with consistent increases or decreases across the walking conditions. After this step, the spurious correlations were excluded from further distribution analysis. As great care was taken to remove non-neuronal artifacts before the data analyses, neck muscle activity should not account for

the consistently increasing EEG-EMG PSD correlations at the outer-ring EEG channels. Moreover, neck muscle activity mainly affects the EEG channels located on the back of the scalp. The observed EEG channels should be gathered at the back of the scalp if neck muscle activity led to the above finding. However, this was not the case. In this study, we utilized power spectrum correlations to investigate the correlation between EEG and EMG data. This enabled us to explore PSD coupling between the EEG and EMG across gait cycles and frequency bands. In addition, a few other methods, such as coherence and directed transfer function [51], are available to explore the relationship between EEG and EMG.

V. CONCLUSION

In this study, we explored the spectral power densities of EEG and EMG signals and their PSD correlations under four walking conditions performed in identical experimental settings. A wide range of frequencies from delta band to gamma band were involved in walking. The EEG PSD was significantly different in sensorimotor and posterior parietal areas between exoskeleton-assisted walking and non-exoskeleton walking. The EMG PSD representation was affected by the exoskeleton during walking, and there were obvious distinctions between walking without an exoskeleton and walking while wearing the exoskeleton. However, the effects of the exoskeleton on the EMG PSD were much similar among the different walking conditions wherein the exoskeleton was worn. The exploration of EEG-EMG PSD correlations demonstrated that the relationship between the EEG and EMG over gait cycles was altered across the different walking conditions and that the alteration in the EEG-EMG relationship depended on the frequency band. As observed in the EEG signal, the theta band was predominant in the decreasing EEG-EMG PSD correlations and the alpha and beta bands were predominant in the increasing EEG-EMG PSD correlations. There was no predominant frequency band in the EMG signal. Based on the spatial distribution, the TA EMG channel was the most involved in the increasing EEG-EMG PSD correlations and the SM EMG channel was the least involved. Intriguingly, the predominant EEG channels involved in the decreasing EEG-EMG PSD correlations were found over the sensorimotor area, while the predominant EEG channels involved in the increasing EEG-EMG PSD correlations were scattered around the outer-ring area. This is the first study to address the spatial distributions relevant to walking from the perspective of the different channels. Our findings add to an expanding body of knowledge regarding EEG and EMG representations associated with ambulation. They may be informative for the development of a more human-compatible assistive exoskeleton and new locomotor rehabilitation techniques with gait orthosis.

REFERENCES

[1] J. F. Veneman, R. Kruidhof, E. E. G. Hekman, R. Ekkelenkamp, E. H. F. van Asseldonk, and H. van der Kooij, "Design and evaluation of the LOPES exoskeleton robot for interactive gait rehabilitation," *IEEE Trans. Neural Syst. Rehabil. Eng.*, vol. 15, no. 3, pp. 379–386, Sep. 2004.

[2] Y. Liu, M. Li, H. Zhang, H. Wang, J. Li, J. Jia, Y. Wu, and L. Zhang, "A tensor-based scheme for stroke patients' motor imagery EEG analysis in BCI-FES rehabilitation training," *J. Neurosci. Methods*, vol. 222, pp. 238–249, Jan. 2014.

[3] G. Pfurtscheller, C. Neuper, D. Flotzinger, and M. Pregenzerb, "EEG-based discrimination between imagination of right and left hand movement," *Electroencephalogr. Clin. Neurophysiol.*, vol. 103, no. 6, pp. 642–651, Dec. 1997.

[4] H. Ramoser, J. Müller-Gerking, and G. Pfurtscheller, "Optimal spatial filtering of single trial EEG during imagined hand movement," *IEEE Trans. Neural Syst. Rehabil. Eng.*, vol. 8, no. 4, pp. 441–446, Dec. 2000.

[5] G. Tacchino, M. Gandolla, S. Coelli, R. Barbieri, A. Pedrocchi, and A. M. Bianchi, "EEG analysis during active and assisted repetitive movements: Evidence for differences in neural engagement," *IEEE Trans. Neural Syst. Rehabil. Eng.*, vol. 25, no. 6, pp. 761–771, Jun. 2017.

[6] M. Severens, M. Perusquia-Hernandez, B. Nienhuis, J. Farquhar, and J. Duysens, "Using actual and imagined walking related desynchronization features in a BCI," *IEEE Trans. Neural Syst. Rehabil. Eng.*, vol. 23, no. 5, pp. 877–886, Sep. 2015.

[7] M. Wieser, J. Haefeli, and L. Bütler, L. Jäncke, R. Riener, and S. Koeneke, "Temporal and spatial patterns of cortical activation during assisted lower limb movement," *Experim. Brain Res.*, vol. 203, no. 1, pp. 181–191, May 2010.

[8] B. H. Dobkin, A. Firestine, M. West, K. Saremi, and R. Woods, "Ankle dorsiflexion as an fMRI paradigm to assay motor control for walking during rehabilitation," *NeuroImage*, vol. 23, no. 1, pp. 370–381, 2004.

[9] C. Calautti and J.-C. Baron, "Functional neuroimaging studies of motor recovery after stroke in adults," *Stroke*, vol. 34, no. 6, pp. 1553–1566, 2003.

[10] M. Gandolla, N. S. Ward, F. Molteni, E. Guanziroli, G. Ferrigno, and A. Pedrocchi, "The neural correlates of long-term carryover following functional electrical stimulation for stroke," *Neural Plasticity*, vol. 2016, Nov. 2016, Art. no. 4192718.

[11] I. Miyai, H. C. Tanabe, I. Sase, H. Eda, I. Oda, I. Konishi, Y. Tsunazawa, T. Suzuki, T. Yanagida, and K. Kubota, "Cortical mapping of gait in humans: A near-infrared spectroscopic topography study," *NeuroImage*, vol. 14, no. 5, pp. 1186–1192, 2001.

[12] J. Wagner, T. Solis-Escalante, P. Grieshofer, C. Neuper, G. Müller-Putz, and R. Scherer, "Level of participation in robotic-assisted treadmill walking modulates midline sensorimotor EEG rhythms in able-bodied subjects," *NeuroImage*, vol. 63, no. 3, pp. 1203–1211, Nov. 2012.

[13] T. P. Luu, J. A. Brantley, S. Nakagome, F. Zhu, and J. L. Contreras-Vidal, "Electrocortical correlates of human level-ground, slope, and stair walking," *PLoS ONE*, vol. 12, no. 11, Nov. 2017, Art. no. e0188500.

[14] G. R. Müller-Putz, D. Zimmermann, B. Graimann, K. Nestinger, G. Korisek, and G. Pfurtscheller, "Event-related beta eeg-changes during passive and attempted foot movements in paraplegic patients," *Brain Res.*, vol. 1137, pp. 84–91, Mar. 2007.

[15] J. T. Gwin, K. Gramann, S. Makeig, and D. P. Ferris, "Electrocortical activity is coupled to gait cycle phase during treadmill walking," *NeuroImage*, vol. 54, no. 2, pp. 1289–1296, 2011.

[16] J. Wagner, T. Solis-Escalante, R. Scherer, C. Neuper, and G. Müller-Putz, "It's how you get there: Walking down a virtual alley activates premotor and parietal areas," *Frontiers Hum. Neurosci.*, vol. 8, p. 93, Feb. 2014.

[17] J. Wagner, X. S. Makeig, M. Gola, C. Neuper, and G. Mu, "Distinct β band oscillatory networks subserving motor and cognitive control during gait adaptation," *J. Neurosci.*, vol. 36, no. 7, pp. 2212–2226, Feb. 2016.

[18] A. R. Sipp, J. T. Gwin, S. Makeig, and D. P. Ferris, "Loss of balance during balance beam walking elicits a multifocal theta band electrocortical response," *J. Neurophysiol.*, vol. 110, no. 9, pp. 2050–2060, Aug. 2013.

[19] M. Seeber, R. Scherer, J. Wagner, T. Solis-Escalante, and G. R. Müller-Putz, "EEG beta suppression and low gamma modulation are different elements of human upright walking," *Frontiers Hum. Neurosci.*, vol. 8, p. 485, Jul. 2014.

[20] M. Seeber, R. Scherer, J. Wagner, T. Solis-Escalante, and G. R. Müller-Putz, "High and low gamma EEG oscillations in central sensorimotor areas are conversely modulated during the human gait cycle," *NeuroImage*, vol. 112, pp. 318–326, May 2015.

[21] T. Castermans, M. Duvinage, G. Cheron, and T. Dutoit, "About the cortical origin of the low-delta and high-gamma rhythms observed in EEG signals during treadmill walking," *Neurosci. Lett.*, vol. 561, pp. 166–170, Feb. 2014.

[22] K. L. Snyder, J. E. Kline, H. J. Huang, and D. P. Ferris, "Independent component analysis of gait-related movement artifact recorded using EEG electrodes during treadmill walking," *Frontiers Hum. Neurosci.*, vol. 9, p. 639, Dec. 2015.
[23] J. E. Kline, H. J. Huang, K. L. Snyder, and D. P. Ferris, "Isolating gait-related movement artifacts in electroencephalography during human walking," *J. Neural Eng.*, vol. 12, no. 4, 2015, Art. no. 046022.
[24] K. Nathan and J. L. Contreras-Vidal, "Negligible motion artifacts in scalp electroencephalography (EEG) during treadmill walking," *Frontiers Hum. Neurosci.*, vol. 9, p. 708, Jan. 2016.
[25] Y. Hashimoto, J. Ushiba, A. Kimura, M. Liu, and Y. Tomita, "Correlation between EEG-EMG coherence during isometric contraction and its imaginary execution," *Acta Neurobiologiae Experimentalis*, vol. 70, no. 1, pp. 76–85, Feb. 2010.
[26] V. Chakarov, J. R. Naranjo, J. Schulte-Mönting, W. Omlor, F. Huethe, and R. Kristeva, "Beta-range EEG-EMG coherence with isometric compensation for increasing modulated low-level forces," *J. Neurophysiol.*, vol. 102, no. 2, pp. 1115–1120, Aug. 2009.
[27] A. Presacco, R. Goodman, L. Forrester, and J. L. Contreras-Vidal, "Neural decoding of treadmill walking from noninvasive electroencephalographic signals," *J. Neurophysiol.*, vol. 106, no. 4, pp. 1875–1887, Jul. 2011.
[28] A. Presacco, L. W. Forrester, and J. L. Contreras-Vidal, "Decoding intralimb and inter-limb kinematics during treadmill walking from scalp electroencephalographic (EEG) signals," *IEEE Trans. Neural Syst. Rehabil. Eng.*, vol. 20, no. 2, pp. 212–219, Mar. 2012.
[29] Y. Ding, I. Galiana, A. T. Asbeck, S. M. M. De Rossi, J. Bae, T. R. T. Santos, V. L. de Araujo, S. Lee, K. G. Holt, and C. Walsh, "Biomechanical and physiological evaluation of multi-joint assistance with soft exosuits," *IEEE Trans. Neural Syst. Rehabil. Eng.*, vol. 25, no. 2, pp. 119–130, Feb. 2017.
[30] Y. He, K. Nathan, A. Venkatakrishnan, R. Rovekamp, C. Beck, R. Ozdemir, G. E. Francisco, and J. L. Contreras-Vidal, "An integrated neuro-robotic interface for stroke rehabilitation using the NASA X1 powered lower limb exoskeleton," in *Proc. 36th Annu. Int. Conf. IEEE Eng. Med. Biol. Soc.*, Aug. 2014, pp. 3985–3988.
[31] H. Stolze, J. P. Kuhtz-Buschbeck, C. Mondwurf, A. Boczek-Funcke, K. Jöhnk, G. Deuschl, and M. Illert, "Gait analysis during treadmill and overground locomotion in children and adults," *Electroencephalogr. Clin. Neurophysiol./Electromyography Motor Control*, vol. 105, no. 6, pp. 490–497, Dec. 1997.
[32] H. Yu, M. S. Cruz, G. Chen, S. Huang, C. Zhu, E. Chew, Y. S. Ng, and N. V. Thakor, "Mechanical design of a portable knee-ankle-foot robot," in *Proc. IEEE Int. Conf. Robot. Automat.*, May 2013, pp. 2183–2188.
[33] G. Chen, P. Qi, Z. Guo, and H. Yu, "Mechanical design and evaluation of a compact portable knee–ankle–foot robot for gait rehabilitation," *Mechanism Mach. Theory*, vol. 103, pp. 51–64, Sep. 2016.
[34] J. Li, G. Chen, P. Thangavel, H. Yu, N. Thakor, A. Bezerianos, and Y. Sun, "A robotic knee exoskeleton for walking assistance and connectivity topology exploration in EEG signal," in *Proc. 6th IEEE Int. Conf. Biomed. Robot. Biomechtron. (BioRob)*, Jun. 2016, pp. 1068–1073.
[35] E. Criswell, *Cram's Introduction to Surface Electromyography*. Burlington, MA, USA: Jones & Bartlett Publishers, 2010.
[36] G. Allison, R. N. Marshall, and K. P. Singer, "EMG signal amplitude normalization technique in stretch-shortening cycle movements," *J. Electromyography Kinesiology*, vol. 3, no. 4, pp. 236–244, 1993.
[37] K. J. Netto and A. F. Burnett, "Reliability of normalisation methods for EMG analysis of neck muscles," *Work*, vol. 26, no. 2, pp. 123–130, 2006.
[38] A. Delorme and S. Makeig, "EEGLAB: An open source toolbox for analysis of single-trial EEG dynamics including independent component analysis," *J. Neurosci. Methods*, vol. 134, no. 1, pp. 9–21, Mar. 2004.
[39] G. Kaur, A. S. Arora, and V. Jain, "Comparison of the techniques used for segmentation of EMG signals," in *Proc. 11th WSEAS Int. Conf. Math. Comput. Methods Sci. Eng.*, Nov. 2009, pp. 124–129.
[40] P. He, G. Wilson, and C. Russell, "Removal of ocular artifacts from electroencephalogram by adaptive filtering," *Med. Biol. Eng. Comput.*, vol. 42, no. 3, pp. 407–412, 2004.
[41] J. Li, Y. Chen, F. Taya, J. Lim, K. Wong, Y. Sun, and A. Bezerianos, "A unified canonical correlation analysis-based framework for removing gradient artifact in concurrent EEG/fMRI recording and motion artifact in walking recording from EEG signal," *Med. Biol. Eng. Comput.*, vol. 55, no. 9, pp. 1669–1681, Sep. 2017.
[42] B. Feige, A. Aertsen, and R. Kristeva-Feige, "Dynamic synchronization between multiple cortical motor areas and muscle activity in phasic voluntary movements," *J. Neurophysiol.*, vol. 84, no. 5, pp. 2622–2629, Nov. 2000.
[43] J. A. Brantley, T. P. Luu, R. Ozdemir, F. Zhu, A. T. Winslow, H. Huang, and J. L. Contreras-Vidal, "Noninvasive EEG correlates of overground and stair walking," in *Proc. 38th Annu. Int. Conf. IEEE Eng. Med. Biol. Soc. (EMBC)*, Aug. 2016, pp. 5729–5732.
[44] R. Merletti and P. Di Torino, "Standards for reporting EMG data," *J. Electromyogr. Kinesiol.*, vol. 9, no. 1, pp. 3–4, 1999.
[45] B. H. Bland and S. D. Oddie, "Theta band oscillation and synchrony in the hippocampal formation and associated structures: The case for its role in sensorimotor integration," *Behavioural Brain Res.*, vol. 127, nos. 1–2, pp. 119–136, Dec. 2001.
[46] A. J. del Ama and G. Asín-Prieto, E. Piñuela-Martín, S. Pérez-Nombela, V. Lozano-Berrio, D. Serrano-Muñóz, F. Trincado-Alonso, J. González-Vargas, Á. Gil-Agudo, J. L. Pons, and J. C. Moreno, "Muscle activity and coordination during robot-assisted walking with H2 exoskeleton," in *Converging Clinical and Engineering Research on Neurorehabilitation II*. Cham, Switzerland: Springer, 2017, pp. 349–353.
[47] M. Seeber, R. Scherer, and G. R. Müller-Putz, "EEG oscillations are modulated in different behavior-related networks during rhythmic finger movements," *J. Neurosci.*, vol. 36, no. 46, pp. 11671–11681, 2016.
[48] S. N. Baker, E. Olivier, and R. N. Lemon, "Coherent oscillations in monkey motor cortex and hand muscle EMG show task-dependent modulation," *J. Physiol.*, vol. 501, no. 1, pp. 225–241, 1997.
[49] J. T. Gwin and D. P. Ferris, "Beta- and gamma-range human lower limb corticomuscular coherence," *Frontiers Hum. Neurosci.*, vol. 6, p. 258, Sep. 2012.
[50] T. H. Petersen, M. Willerslev-Olsen, B. A. Conway, and J. B. Nielsen, "The motor cortex drives the muscles during walking in human subjects," *J. Physiol.*, vol. 590, no. 10, pp. 2443–2452, Oct. 2012.
[51] F. Artoni, C. Fanciullacci, F. Bertolucci, A. Panarese, S. Makeig, S. Micera, and C. Chisari, "Unidirectional brain to muscle connectivity reveals motor cortex control of leg muscles during stereotyped walking," *NeuroImage*, vol. 159, pp. 403–416, Oct. 2017.

JUNHUA LI received the Ph.D. degree in computer science from the Department of Computer Science and Engineering, Shanghai Jiao Tong University, China, in 2013.

He is currently a Lecturer with the School of Computer Science and Electronic Engineering, University of Essex, Colchester, U.K. He was a Senior Research Fellow with the National University of Singapore, Singapore. His research interests include brain–computer interface, computational neuroscience, data analytics, and machine learning.

GEORGIOS N. DIMITRAKOPOULOS received the Ph.D. degree from the Department of Electrical and Computer Engineering, University of Patras, Greece, in 2018.

He was a Research Assistant with the Singapore Institute for Neurotechnology, National University of Singapore, Singapore. He is currently a Postdoctoral Researcher with the University of Patras and FORTH/ICE-HT, Patras, Greece. His research interests include machine learning and network analysis with applications in systems biology and neuroscience fields.

PAVITHRA THANGAVEL received the master's degree in biomedical engineering from VIT University, India, in 2016.

She was a Researcher with the Biorobotics Laboratory, National University of Singapore, Singapore. Her research interests include the implementation of the experiments and data analysis.

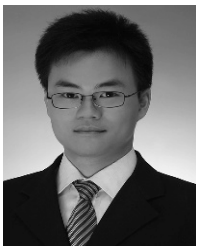

GONG CHEN received the B.E. degree from Shanghai Jiao Tong University, Shanghai, China, in 2011, with a focus on mechanical engineering and automation and computer science, and the Ph.D. degree in biomedical engineering from the University of Singapore, in 2016.

He is currently a Research Fellow with the National University of Singapore. His current research interests include rehabilitation robots systems, compliant actuator, and brain–computer interface.

YU SUN received the B.Eng. degree in biomedical engineering from the Nanjing University of Aeronautics and Astronautics, China, in 2005, the Ph.D. degree in electronic, electrical, and system engineering from Loughborough University, U.K., in 2011, and the joint Ph.D. degree in biomedical engineering from Shanghai Jiao Tong University, China, in 2012. From 2012 to 2017, he was a Postdoctoral Research Fellow and a Senior Research Fellow with the Centre for Life Sciences, National University of Singapore, Singapore. He is currently a Research Professor with the Key Laboratory for Biomedical Engineering of Ministry of Education of China, Zhejiang University. His research emphasis has been placed on the integration of the neural engineering, cognitive sciences, and neuroergonomics in service of insights into functions of the brain, cognition, and behavior. He has led more than 80 peer-reviewed articles and proceeding articles. His research interests include multimodal brain connectome, passive brain–computer interface, brain state monitoring, and temporal brain network analysis. He has been a Youth Committee Member of the Chinese Society of Digital Medicine, since 2018. He was a recipient of the Best Poster Award of the IEEE Life Science Grand Challenge Conference 2013 (IEEE LSGCC). He has been serving as an Associate Editor for the *Medical & Biological Engineering & Computing* journal, since 2016, and a Corresponding Expert for the journal *Engineering*, since 2019.

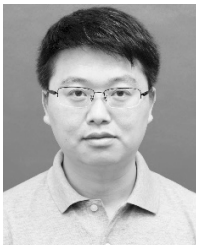

ZHAO GUO received the Ph.D. degree in mechatronics engineering from the Institute of Robotics, Shanghai Jiao Tong University, China, in 2012.

From 2012 to 2015, he was a Research Fellow with the Department of Biomedical Engineering, National University of Singapore (NUS), Singapore. He is currently an Associate Professor with the School of Power and Mechanical Engineering, Wuhan University, China. His research interests include compliant actuator, design and control of exoskeleton, and physical human–robot interaction. He mainly focuses on the area of rehabilitation robotics.

HAOYONG YU received the B.S. and M.S. degrees from Shanghai Jiao Tong University, Shanghai, China, in 1988 and 1991, respectively, and the Ph.D. degree from the Massachusetts Institute of Technology, Cambridge, MA, USA, in 2002, all in mechanical engineering.

He is currently an Associate Professor with the Department of Biomedical Engineering, National University of Singapore. His research interests include medical robotics, rehabilitation engineering and assistive technologies, and system dynamics and control.

NITISH V. THAKOR was the Founding Director of the Singapore Institute for Neurotechnology (SINAPSE), National University of Singapore and Biomedical Engineering, from 2012 to 2018. He has been a Professor of biomedical engineering and electrical and computer engineering with Johns Hopkins University, since 1983. He has published 395 refereed journal articles. His technical expertise is in the field of neuroengineering, where he has pioneered many technologies for brain monitoring to prosthetic arms and neuroprosthesis. He is also a Fellow of the American Institute of Medical and Biological Engineering and the International Federation of Medical and Biological Engineering and a Founding Fellow of the Biomedical Engineering Society. He was a recipient of the Research Career Development Award from the National Institutes of Health, the Presidential Young Investigator Award from the National Science Foundation, the Academic Career Award and the Technical Excellence in Neuroengineering from the IEEE Engineering in Medicine and Biology Society, the Distinguished Alumnus Award from the Indian Institute of Technology, Bombay, India, and the Centennial Medal from the School of Engineering, University of Wisconsin. He was the Editor-in-Chief of the IEEE TNSRE, from 2005 to 2011. He is also the Editor-in-Chief of *Medical and Biological Engineering and Computing*.

ANASTASIOS BEZERIANOS received the degree in physics from Patras University, the degree in telecommunications from Athens University, and the Ph.D. degree in bioengineering from the University of Patras. He is currently the Head of the Cognitive Engineering (COGEN) Laboratory, N.1 Health Institute, National University of Singapore, a Professor with the NUS Graduate School for Integrative Sciences and Engineering, and a Visiting Professor with the Computer Science Department, New South Wales University (NSWU), Canberra, Australia. He has been a Professor of medical physics with the Medical School of Patras University, Patras, Greece, since 2004. His research entails diverse areas spanning from artificial intelligence and robotics to biomedical signal processing and brain imaging as well as mathematical biology and systems medicine and bioinformatics. His work is summarized in 140 journals and 217 conference proceedings publications, one book, and two patents. He has research collaborations with research institutes and universities in Japan, China, and Europe. He is also a Fellow of the European Alliance for Medical and biological Engineering and Science (EAMBES), and the Founder and the Chairman of the Biannual International Summer School on Emerging Technologies in biomedicine. He is also an Associate Editor of the IEEE TNSRE and the *PLOS ONE Neuroscience* journals and a Reviewer for several international scientific journals. He is also a Registered Expert of the Horizon 2020 program of the European Union and a Reviewer of research grant proposals in Greece, Italy, Cyprus, and Canada.